NANO LETTERS

2006
Vol. 6, No. 7
1479−1482

Electric-Field-Assisted Assembly of Perpendicularly Oriented Nanorod Superlattices

Kevin M. Ryan,[‡,§] Alex Mastroianni,[†] Kimani A. Stancil,[‡] Haitao Liu,[†] and A. P. Alivisatos*[,†,‡]

Department of Chemistry, University of California, and Materials Science Division, Lawrence Berkeley National Laboratory, Berkeley, California 94720

Received April 18, 2006; Revised Manuscript Received May 15, 2006

ABSTRACT

We observe the assembly of CdS nanorod superlattices by the combination of a DC electric field and solvent evaporation. In each electric-field (1 V/μm) assisted assembly, CdS nanorods (5 nm $\times$ 30 nm) suspended initially in toluene were observed to align perpendicular to the substrate. Azimuthal alignment along the nanorod crystal faces and the presence of stacking faults indicate that both 2D and 3D assemblies were formed by a process of controlled super crystal growth.

Self-assembly or directed assembly of discrete nanostructures into organized patterns provides a new route to the formation of functional materials. Colloidal nanocrystals are suitable building blocks because they can be synthesized with size and shape control.[1] The assembly of symmetrical nanospheres and nanocubes into superlattices is known; and in the case of silver nanocrystals, 3 nm in diameter, an insulator to metal transition is observed to occur as a function of sphere size and interparticle separation.[2−4] In effect, the superlattice functions as a novel nanocrystal solid where it is possible to control the electronic coupling by manipulating the size and position of the quantum confined structural units. The coupling can be modified further through exchange of the insulating organic ligands on the nanocrystal surface with low barrier organics, for example, hydrazine. Talapin and Murray used this approach to convert poorly conducting PbSe nanocrystal solids into n-and p-channel field-effect transistors.[5] The ability to direct anisotropic structures such as cylindrical nanorods into superlattices is less well developed but also interesting. In organized nanorod superlattices, it may be possible to simultaneously and independently optimize quantities that depend on the diameter (such as band gap) from quantities that depend on length (total absorption, cross section, or conductivity).

Superlattice formation with spherical nanocrystals is strongly correlated to size monodispersity and their entropy-driven packing under slow evaporation conditions. Although dimensional control and monodispersity in nanorods has been achieved, their organization into superlattices is restricted because both positional and orientational ordering is required during assembly. Some progress has been made in preferential nanorod alignment in single layers with nematic and smectic ordering achieved from gentle evaporation of low-boiling-point solvents.[6−9] The rods align parallel to substrate in small domain sizes. There is further evidence for orientation of anisotropic nanostructured rods, tubes, and wires along electric field lines. The strength of the interaction is greatest in metallic nanostructures followed by nanostructures with permanent dipole moments, for example, CdSe and CdS nanorods.[10,11] Anisotropic structures with low polarizability, such as silicon nanowires and carbon nanotubes, can also be induced to align when the electric-field-induced torque is greater than the thermal excitation energy (kT).[12−16] The effect is usually observed when a solution of 1D nanostructures is deposited between interdigitated electrodes, resulting in orientation along field lines parallel to the substrate with no positional order.

In our research, we have used the combination of a DC electric field and slow evaporation of solvent (toluene) to generate superlattices of II−VI semiconductor nanorods with orientation perpendicular to a substrate (As this work was in progress, we received notice of similar unpublished work from the laboratories of Professor T. Russell and T. Emrick of U. Mass. Amherst.) CdS nanorods (30 nm $\times$ 5 nm) were formed by the injection of sulfur/tri-*n*-octylphosphine solutions at high temperature into hot cadmium oxide/surfactant mixtures.[17] The solution of size monodisperse CdS nanorods

* To whom correspondence should be addressed. E-mail: alivis@uclink4.berkeley.edu.
† Department of Chemistry, University of California.
‡ Materials Science Division, Lawrence Berkeley National Laboratory.
§ Permanent address: Materials and Surface Science Institute, University of Limerick, Limerick, Ireland.

10.1021/nl060866o CCC: $33.50
Published on Web 06/21/2006

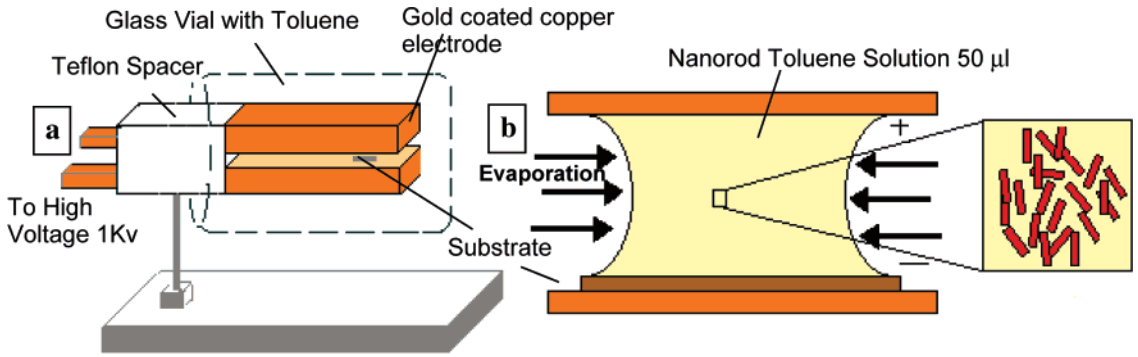

Figure 1. Schematic of electrode assembly for nanorod alignment. (a) 3D drawing. Each electrode measures 35 mm × 15 mm × 5 mm and is separated at a distance of 1.2 mm. The electrode assembly in a horizontal orientation is placed in a glass vial with 1 mL of toluene to create a saturated atmosphere. (b) 2D close up of trapped meniscus. The substrate (carbon-coated electron microscopy grid or silicon nitride membrane window) is placed between the electrodes, and 50 μL of nanorod toluene solution is deposited forming a meniscus between the upper and lower electrode.

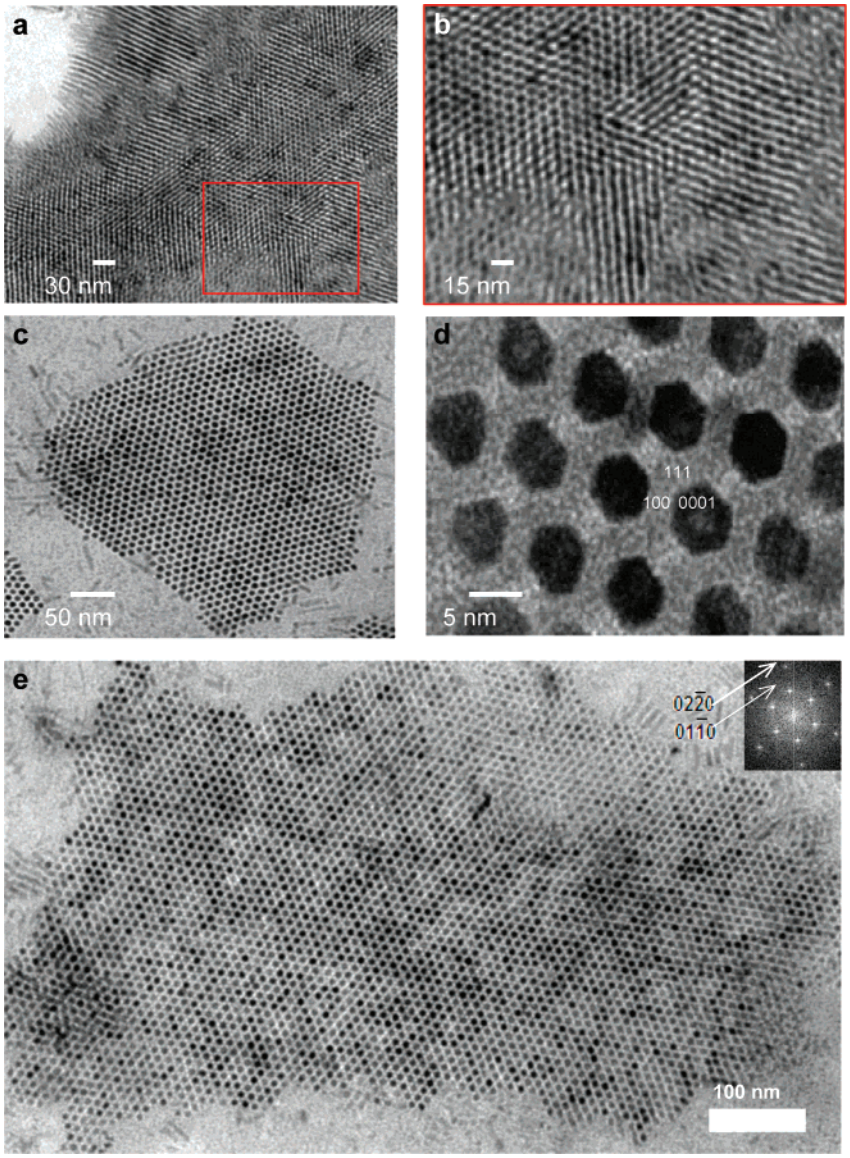

Figure 2. TEM images of perpendicularly aligned nanorod superlattices. (a) Section of CdS nanorod (30 nm × 5 nm) domain in absence of electric field, scale bar = 30 nm. (b) Magnified section of a, showing parallel to perpendicular alignment from edge to center (scale bar = 15 nm). (c) CdS nanorods aligned under a field of 1 V/μm. (d) Azimuthal alignment of the nanorods. (e) 30 nm CdS nanorod superlattice with domain size >0.5 μm^2; inset: Fourier transform of image showing electron diffraction from hexagonally ordered 2D array. Maxima highlighted from [01−10] and [02−20] diffraction planes with remaining planes [10−10], [1−100], [0−110], [−1010], [−1100] and [20−20], [2−200], [0−220], [−2020], [−2200] clockwise from these positions, respectively.

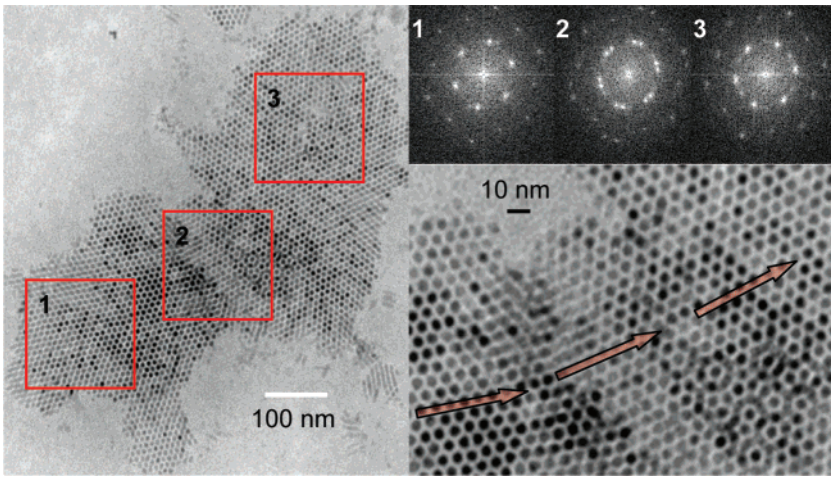

Figure 3. Electron diffraction from selected regions of electric-field-assisted perpendicularly aligned nanorod domain showing superlattice stacking fault.

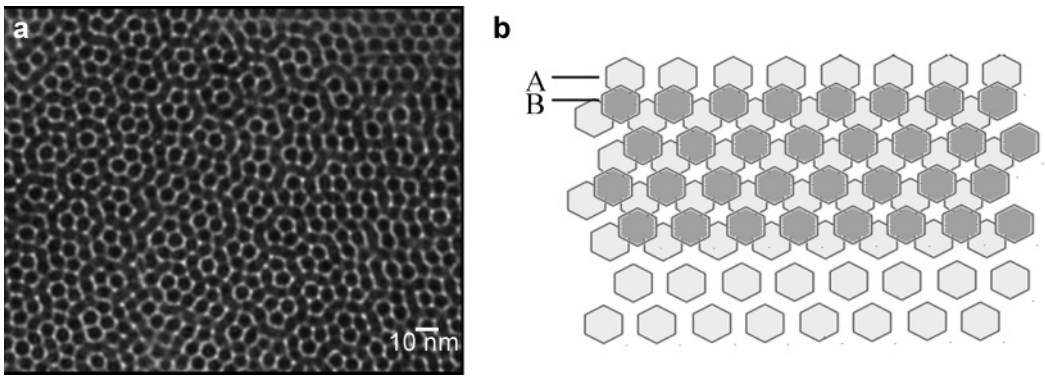

Figure 4. (a) 3D superlattice of of CdS nanorods 30 nm × 5 nm scale bar = (10 nm), (b) Schematic showing the top down view of perpendicular arrangement of nanorods with AB stacking.

in toluene is trapped between parallel electrodes (Figure 1) and allowed to dry under a DC electric field of 1 V μm^{-1}. Gentle evaporation is achieved through near-saturation of the entire assembly in a toluene atmosphere. The solvent evaporation gradually decreases the diameter of the trapped droplet, packing the nanorods into a 2D supercrystal. In this study, we observe that for a slower rate of the solvent evaporation, a higher degree of positional order is present in our nanorod assemblies.

Figure 2a and b shows a 2D nanorod array evaporated from toluene in the absence of an electric field. The center of the domain consists of perpendicularly aligned rods in a 2D hexagonal array. The outer layers of nanorods progressively tilt toward the center, aligning parallel to the substrate at the domain edge. This tilting of the nanorods from perpendicular to parallel at the edges is in good agreement with alignment observed in condensed 3D nanocrystal solids reported by Talapin.[18] In that work, the progressive perpendicular to parallel tilt over hundreds of multilayers from edge to center was sufficient to rotate the polarization of light as verified using crossed polarizers. Assuming that transmitted polarized light is directed normal to the substrate, the observed birefringence changes with both tilting and rotation of the nanorod with respect to the substrate plane. The densely packed rods in Figure 2a and b demonstrate good positional order with 180° range of disorder in planar orientation across the nanorod aggregate.

The electric field favors the perpendicular orientation of the rods during the assembly process. The CdS nanorods (30 nm × 5 nm) are estimated to have a permanent dipole moment of ~220 D because of the noncentrosymmetric Wurtzite lattice.[19,20] Additionally, the induced dipole parallel and perpendicular to the long axis were calculated at 182 D and 51 D, respectively.[21] The electric field will act on the nanorods producing rotation about its axis while the evaporating solvent laterally confines them into an array. The net effect is a 2D superlattice of semiconductor nanorods with all the *c* axes aligned normal to the substrate. Figure 2c shows a typical TEM image of a single layer of hexagonally packed nanorods 30 nm × 5 nm showing both positional and orientational order that is extraordinarily resolute throughout the entire domain. The space between the nanorods, 3 nm, is occupied by interdigitated phosphonic acid surfactants. Clearly in the approach described here, the electric field is acting on the nanorods during evaporation to direct high orientational order.

Figure 2d under higher magnification shows the hexagonal faceted ends of the zinc blende nanorod structure. The 2D assembly of the nanorods is also affected by the particle shape where the nanorods demonstrate positional and ori-

entational order as well as azimuthal alignment along their [100] and [111] crystal faces. This azimuthal alignment strongly suggests that super crystallization of hexagonally faceted nanorods is occurring where the total growth rate is slow and each nanorod can dynamically add to or subtract from the growing supercrystal face before locking in. The solvent evaporation assists the close packing of the nanorods as the coordinating surfactant ligands favor the higher entropy of solvation, thereby drawing them into the reducing solvent. The high solubility of octadecylphosphonic acid (ODPA) ligand coordinated nanorods in toluene was evidenced by the lack of sedimentation in bulk solutions over a period of weeks. On this basis, there is little evidence for the preconcentration of nanorods on the substrate before evaporation is complete. This mechanism for superlattice growth is further evidenced in Figure 2e where slower evaporation of nanorods resulted in the formation of superlattice domains $>0.5\ \mu m^2$. The superlattice crystal structure is defect-free throughout the entire domain and the electron diffraction inset shows sharp maxima indexed to the diffraction planes of a hexagonal lattice.

The stacking fault observed in the domain imaged in Figure 3 is further evidence for the controlled sequential addition of nanorods to the growing crystal face of the 2D nanorod superlattice during evaporation. The domain consists of $\sim 4 \times 10^3$ nanorods normal to the substrate. The Fourier transform shows the effective electron diffraction from selected regions of the domain with spot sizes of 200 nm^2. The electron diffraction from region 1 shows a hexagonal superlattice with sharp scattering maxima. Similarly, the electron diffraction from region 3 reflects a hexagonally ordered lattice. The stacking fault is observed in region 2 where the Fourier transform of the image shows two sharp maxima at each position evidencing rotation in the azimuthal alignment occurring at this location. The arrows shown in the magnified image of the defect region are aligned with the [100] crystal planes of the nanorod superlattice clearly showing the stacking fault.

CdS nanorods deposited under an electric field with slow evaporation also demonstrate alignment in three dimensions (Figure 4). 3D nanorod arrays were obtained where the incoming nanorod selectively sits in the interstitial spacing between the nanorods in the underlying layer creating an AB layered 3D superlattice. Figure 4b is a schematic showing how this effect manifests itself as the periodic structure seen in Figure 4a when the two layers are viewed simultaneously in transmission mode. Typically, 3D stacking of nanorods is routinely observed when the concentration of nanorods in solution is high.

The approach described here for assembling superlattices of anisotropic, size- and shape-controlled nanorods normal to a substrate is generally applicable. This level of directional control may prove helpful in the formation of nanorod−polymer solar cells with increased charge-transport efficiencies.[22]

Acknowledgment. This work was supported by the Director, Office of Energy Research, Office of Science, Division of Materials Sciences, of the U.S. Department of Energy under Contract No. DE-AC02-05CH11231. K.A.S would like to thank the Lawrence Postdoctoral Fellowship Program administered under this same DOE Contract. K.M.R. acknowledges financial support from European Union Sixth Framework, Marie Curie Outgoing Fellowship, MOIF-CT-2004-008150 and by AFOSR Grant No. FA9550-04-1-0065. We thank Deborah Aruguete and Steven Hughes for useful discussions.

References

(1) Milliron, D. J.; Hughes, S. M.; Cui, Y.; Manna, L.; Li, J.; Wang, L.-W.; Alivisatos, A. P. *Nature* **2004**, *430*, 190−195.
(2) Dumestre, F.; Chaudret, B.; Amiens, C.; Renaud, P.; Fejes, P. *Science* **2004**, *303*, 821−822.
(3) Markovich, G.; Collier, C. P.; Heath, J. R. *Phys. Rev. Lett.* **1998**, *80*, 3807−3810.
(4) Murray, C. B.; Kagan, C. R.; Bawendi, M. G. *Science* **1995**, *270*, 1335−1338.
(5) Talapin, D. V.; Murray, C. B. *Science* **2005**, *310*, 86−89.
(6) Kim, F.; Kwan, S.; Akana, J.; Yang, P. *J. Am. Chem. Soc.* **2001**, *123*, 4360−4361.
(7) Li, L.-S.; Alivisatos, A. P. *Adv. Mater.* **2003**, *15*, 408−411.
(8) Dumestre, F.; Chaudret, B.; Amiens, C.; Respaud, M.; Fejes, P.; Renaud, P.; Zurcher, P. *Angew. Chem., Int. Ed.* **2003**, *42*, 5213−5216.
(9) Jana, N. R.; Gearheart, L. A.; Obare, S. O.; Johnson, C. J.; Edler, K. J.; Mann, S.; Murphy, C. J. *J. Mater. Chem.* **2002**, *12*, 2909−2912.
(10) Smith, P. A.; Nordquist, C. D.; Jackson, T. N.; Mayer, T. S.; Martin, B. R.; Mbindyo, J.; Mallouk, T. E. *Appl. Phys. Lett.* **2000**, *77*, 1399−1401.
(11) Li, L.-s.; Walda, J.; Manna, L.; Alivisatos, A. P. *Nano Lett.* **2002**, *2*, 557−560.
(12) Joselevich, E.; Lieber, C. M. *Nano Lett.* **2002**, *2*, 1137−1141.
(13) Zhang, Y.; Chang, A.; Cao, J.; Wang, Q.; Kim, W.; Li, Y.; Morris, N.; Yenilmez, E.; Kong, J.; Daj, H. *J. Appl. Phys. Lett.* **2001**, *79*, 3155−3157.
(14) Englander, O.; Christensen, D.; Kim, J.; Lin, L.; Morris, S. J. S. *Nano Lett.* **2005**, *5*, 705−708.
(15) Chung, J.; Lee, K.-H.; Lee, J.; Ruoff, R. S. *Langmuir* **2004**, *20*, 3011−3017.
(16) Fan, D. L.; Zhu, F. Q.; Cammarata, R. C.; Chien, C. L. *Appl. Phys. Lett.* **2004**, *65*, 4175−4177.
(17) Tri-*n*-octylphosphine oxide (Aldrich, 2.73 g), *n*-octadecylphonsphonic acid (Polycarbon, 1.07 g, 3.19 mmol), and CdO (Aldrich, 0.205 g, 1.60 mmol) were added to a three-neck flask. The mixture was degassed at 120 °C for 30 min before it was heated to 320 °C under Ar to dissolve CdO. The temperature was then lowered to 300 °C, and solution of sulfur in tri-*n*-octylphosphine (7.9% w/w, 0.60 g, 1.5 mmol of sulfur) was swiftly injected to the flask via syringe. The nanorod was grown at 290 °C for 30 min. After the reaction, the temperature was lowered to 100 °C and toluene (3−4 mL) was added to dissolve the reaction mixture. The toluene solution was centrifuged at 2500 g to give a yellow precipitate. This precipitate was redissolved in toluene, and the nanorods were precipitated with acetone.
(18) Talapin, D. V.; Shevchenko, E. V.; Murray, C. B.; Kornowski, A.; Förster, S.; Weller, H. *J. Am. Chem. Soc.* **2004**, *126*, 12984.
(19) Krauss, T. D.; University of Rochester, Rochester, NY 14627. Personal communication, 2006.
(20) Li, L.-s.; Alivisatos, A. P. *Phys. Rev. Lett.* **2003**, *90*, 974021−974024.
(21) Böttcher, C. J. F. *Theory of Electric Polarization*; Elsevier: New York, 1973.
(22) Huynh, W. U.; Dittmer, J. J.; Alivisatos, A. P. *Science* **2002**, *295*, 2425−2427.

NL060866O